Recent Highlights on Solid Oxide Cells, Stacks and Modules Developments at CEA

To cite this article: Julie Mouginn *et al* 2023 *ECS Trans.* **111** 1101

View the article online for updates and enhancements.

You may also like

Recent Highlights on Solid Oxide Cells, Stacks and Modules Developments at CEA

J. Mougin[a], J. Laurencin[a] J. Vulliet[b], M. Petitjean[a], E. Grindler[a], S. di Iorio[a], K. Couturier[a], T. Dejob[c], B. Gonzalez[a], G. Cubizolles[a], F. Bosio[a], and J. Aicart[a]

[a] Univ. Grenoble Alpes, CEA/LITEN, 17 rue des Martyrs, 38054 Grenoble, France
[b] CEA/Le Ripault, DMAT, F-37260 Monts, France
[c] Université Paris-Saclay, CEA, 91191, Gif-sur-Yvette, France

Solid Oxide Cell (SOC) technology is considered as an efficient electrolysis technology to produce hydrogen at large scale. It can also operate in fuel cell mode using different fuels (carbon-based or non-carbon based like ammonia), and in reversible mode. Though proofs-of concept have been achieved at different relevant scales for those operating modes, some R&D works still need to be performed to improve performance, durability and cost. Improved and upscaled cells and stacks need to be developed, with a methodology combining multiscale and multiphysics modelling, electrochemical characterization in relevant conditions and advanced post-test analysis. Their integration into modules made of several stacks is also a stepping stone in order to reach multi-MW electrolysers. CEA is working on the whole value chain of SOC technology, from cell development and optimisation to module design and operation through stack upscaling. Recent achievements on those aspects will be presented.

Introduction

Solid Oxide Cell (SOC) technology is a versatile technology able to operate either in electrolysis mode (SOEL), to produce hydrogen at high efficiency, in fuel cell mode (SOFC) using different fuels (carbon-based or non-carbon based like ammonia), in reversible mode (rSOC) with different cycles between electrolysis and fuel cell modes depending on the use case and the type of upstream coupling with renewable energies, and finally in co-electrolysis mode (co-SOEL) to produce syngas out of steam and CO_2.
Though major developments and validations have been performed at relevant scales for those different operating modes, some R&D works still need to be performed to improve performance, durability and cost in a concomitant way, to meet the targeted key performance indicators as set by the EU for instance (1).

CEA is working on SOC technology since more than two decades (Figure 1). Activities have started with exploratory research on ceramic cells including the screening of different types of materials (electrolyte, electrodes) and processes, for SOFC application. In 2005, an important program has started, dedicated to the massive production of hydrogen, coupled to nuclear energy. Several options have been investigated, including several electrolysis technologies but also thermochemical cycles. Scientific activities and techno-economic assessment have demonstrated that SOEL technology was particularly relevant for the production of cost-competitive "low carbon" H_2. In 2014, a lab system was put in

operation, demonstrating the high efficiency achievable with this technology (84%LHV) (2-3). Between 2015 and 2020, an important part of the activity was dedicated to the stack optimization, in terms of both design and process, with the installation of a pilot workshop to reach a high level of reliability of the stacks (4). In March 2021, Genvia company was created, being a joint venture between SLB and CEA, with Vinci, Vicat and ARIS as additional stakeholders. Year 2021 was dedicated to the technology transfer from CEA to Genvia, and the installation of the pilot workshop in Genvia premises. In parallel, R&D activities continued, with upscaling activities, first at cell and stack level, to increase on one hand the size of the cells, from 100 to 200 cm² active area (4), and on the other hand the number of cells per stack, from 25 to 50 and 75 (5-6). Activities on multistack modules design also started, modules made of several stacks being a stepping stone in order to reach multi-MW electrolysers as needed to meet the targets set by the RePowerEU plan intending to install 100 GW of electrolysers in EU in 2030 (7). The technology transfer phase is still ongoing, with still R&D activities jointly performed between CEA and Genvia, while Genvia is preparing the industrial production phase planned to start in 2024. Over those years, a large number of national and European projects supported CEA activities and developments, on the whole value chain, from cells to stacks and systems, and for the different operating modes (SOEL, SOFC, rSOC and co-SOEL). They also allowed developing supporting methodologies like multiscale and multiphysics modelling, advanced microstructural characterization tools and monitoring and diagnostics.
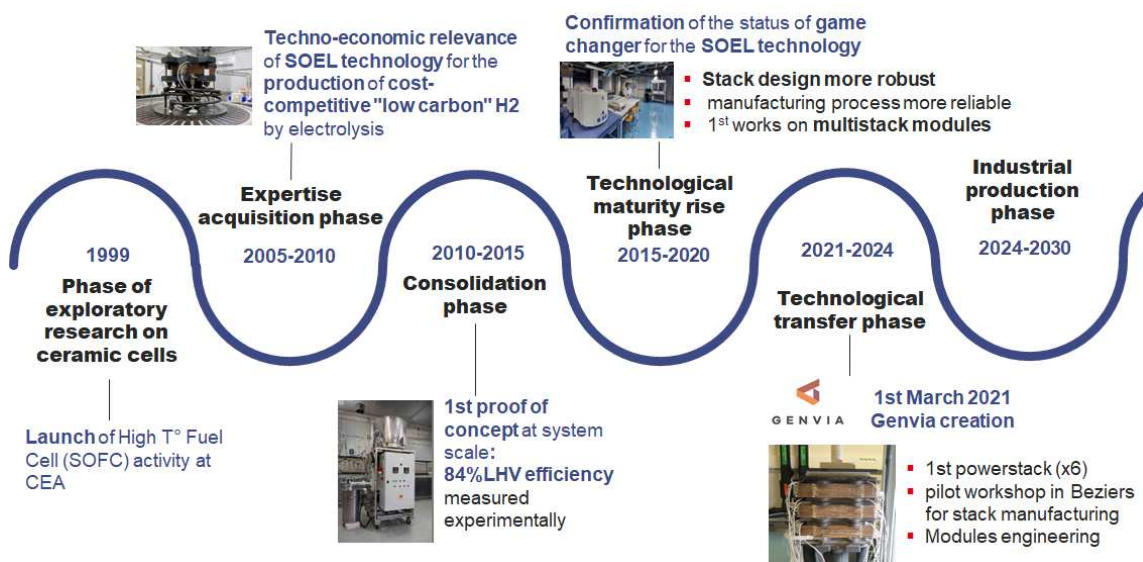

Figure 1. Illustration of the SOC R&D activities performed at CEA over the years.

The present article intends to present the recent achievements obtained at CEA regarding performance and durability at the different scales of cells, stacks and modules. Regarding cells, developments performed to produce cells with improved performances and a larger surface will be reported, with a methodology combining multiscale and multiphysics modelling, electrochemical characterization in relevant conditions and post-test analysis. As far as stack developments are concerned, CEA continued its program on upscaling, and long-term test on a large stack will be reported. In parallel, improved seals are developed to increase the stack robustness to transient operation and interconnect coatings are studied using different deposition techniques. Those components have been first validated at sample scale before integrating some of them into short stacks and full-stacks for validation in real configuration. For instance, the integration of interconnect

protective coatings in short stacks has been evaluated over 5000 h of operation. Finally, a 4-stack module has been developed and put in operation. Made of 4 stacks, each comprising 25 cells of 100 cm² active area, it is able to operate in electrolysis, fuel cell and reversible mode. The first results of its operation will be presented.

Results

<u>Cells</u>

Regarding SOC cells, CEA has developed electrode supported cells, in order to be able to reach high current densities. The hydrogen electrode consists of a ~360 μm Ni/3YSZ support layer and a ~20-25 μm Ni/8YSZ fuel active layer. The electrolyte is a ~ 6-8 μm 8YSZ (8 mol% yttria stabilized zirconia) electrolyte on top of which a CGO (gadolinia doped ceria) barrier layer is deposited. The oxygen electrode is a ~10-25 μm thick composite electrode LSCF-CGO, with a contact layer made of pure LSCF (lanthanum strontium iron cobaltite).

A multiscale and multiphysics model has been developed at CEA to unravel the underlying processes involved in the cell operation and degradation (8-10). The model is used to propose a deep understanding of the reaction mechanisms that take place in the electrodes (11-13). Combined with advanced post-test characterizations (14), it also allows investigating the main degradation phenomena such as the Ni migration in electrolysis mode (15,16). Among different applications, the model can be used to optimize the electrode microstructure to enhance the cell efficiency and robustness. As an illustration, the model has been applied to predict the behavior of the LSCF-CGO composite used as oxygen electrode (17-18). FIB-SEM 3D reconstructions of the microstructures have been performed which allowed to refine and adjust the parameters of the model for electrochemical kinetics using experimental i-V curves and impedance spectra (19). A digital twin of the oxygen electrode has been emulated (20) and a large range of numerical microstructures has been generated for microstructural correlations (less time consuming and less costly than real microstructures) (21). Therefore modifications of oxygen electrode composition (ratio CGO/(LSCF-CGO)), porosity, particle size distribution have been investigated, enabling to define the optimum parameters (figure 2a). More generally, the microstructure of the electrodes and the interfaces have been optimized (reduced mean size particles of the used powders < 1μm, large porosity of the functional electrodes (~46% for the O_2 electrode for example)) to improve the cell performances (figure 2b). As a consequence, the density of triple phase boundaries (TPB) of the LSCF/CGO electrode obtained was very high (17.81×10^{12} μm^{-2}), explaining the good electrochemical performances of this optimized cell. For a cell as depicted in figure 2b, having an optimized oxygen electrode as compared to the reference one, the current density at 1.3 V is increased by roughly 15% for both flow rates considered (figure 2c), exceeding – 1.25 A cm^{-2} for the lowest flow rate (80% steam conversion) at 800 °C.
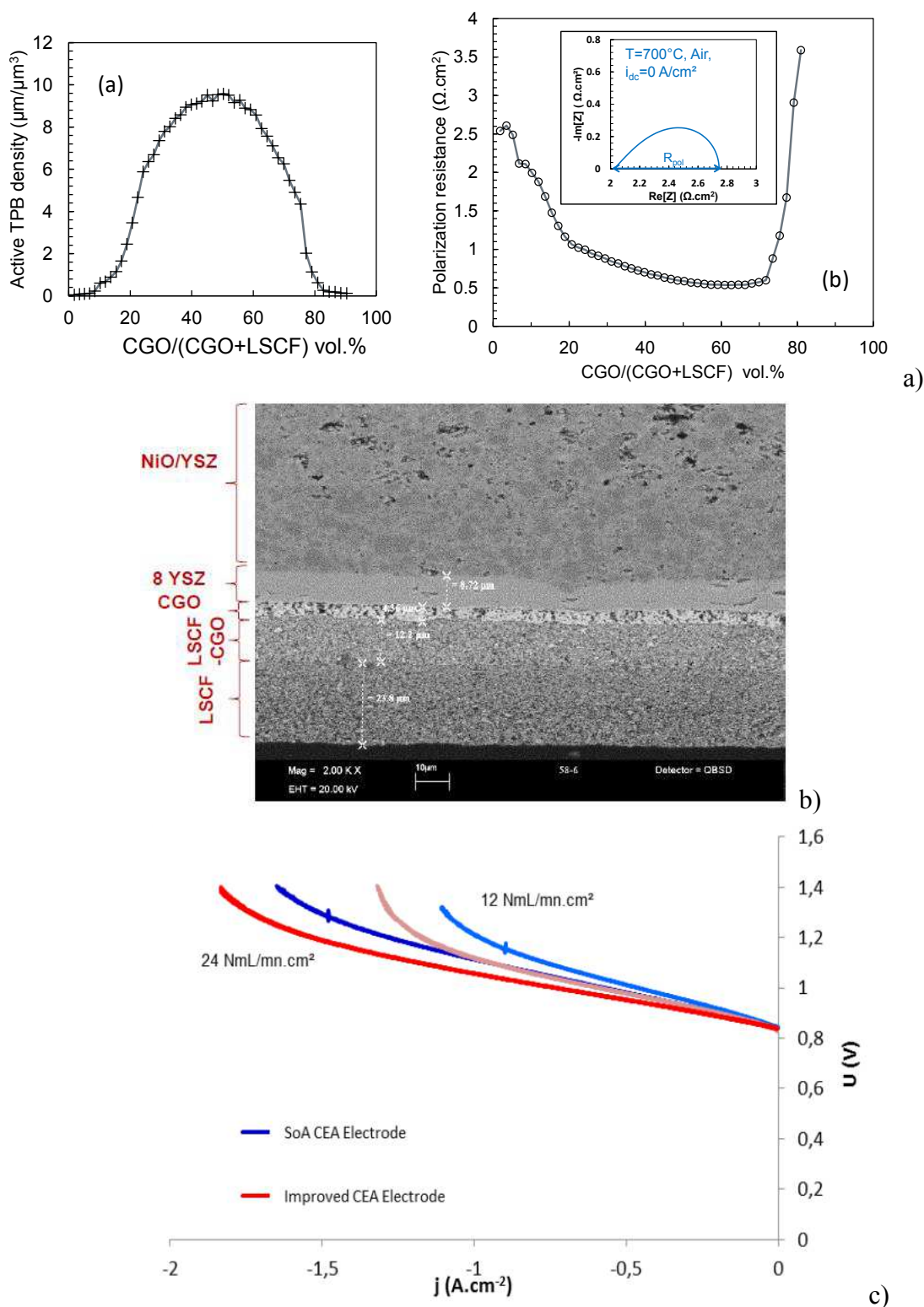
Figure 2. a) TPB (triple phase boundaries) density vs ratio CGO/(LSCF-CGO) (left) and polarisation resistance vs ratio CGO/(LSCF-CGO) (right); b) cross section of the as-produced optimized electrode supported cell, where all layers are visible (fuel electrode, electrolyte, barrier layer between oxygen electrode and electrolyte, and oxygen electrode); c) i-V curve of an optimized single cell including improved electrodes, and comparison to a state of the art (SoA) cell; curves recorded at 800 °C, total flow rate of 12 or 24 NmL min^{-1} cm^{-2} of 90/10 vol.% H_2O/H_2 mix at the fuel electrode, air on the other side.

Besides the efforts performed to improve the intrinsic cells performances presented above, the process has been optimised to obtain a good reproducibility on performances among cells (Figure 3). A current density of – 0.8 A cm^{-2} has been reached at the thermoneutral voltage at 700 °C. Works are in progress on the electrodes microstructures and interfaces to further increase the performances.
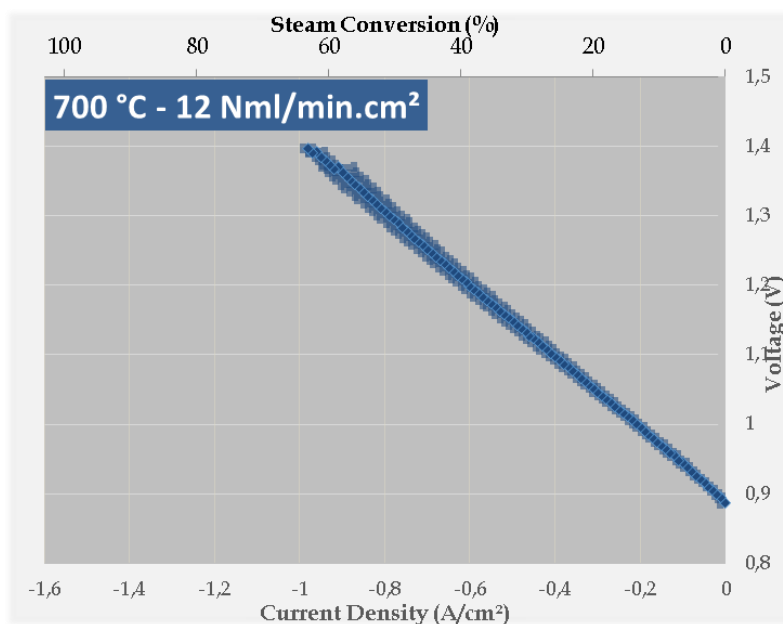

Figure 3. i-V curve of several cells (9 cm² active area); T=700 °C, total flow rate 12 NmL min^{-1} cm^{-2} of 90/10 vol.% H_2O/H_2 mix at the fuel electrode, air on the other side.

After validation at single cell level (9 cm²), cells of 100 cm² and 200 cm² active area have been produced with a good reproducibility (figure 4) and validated at short stack level.
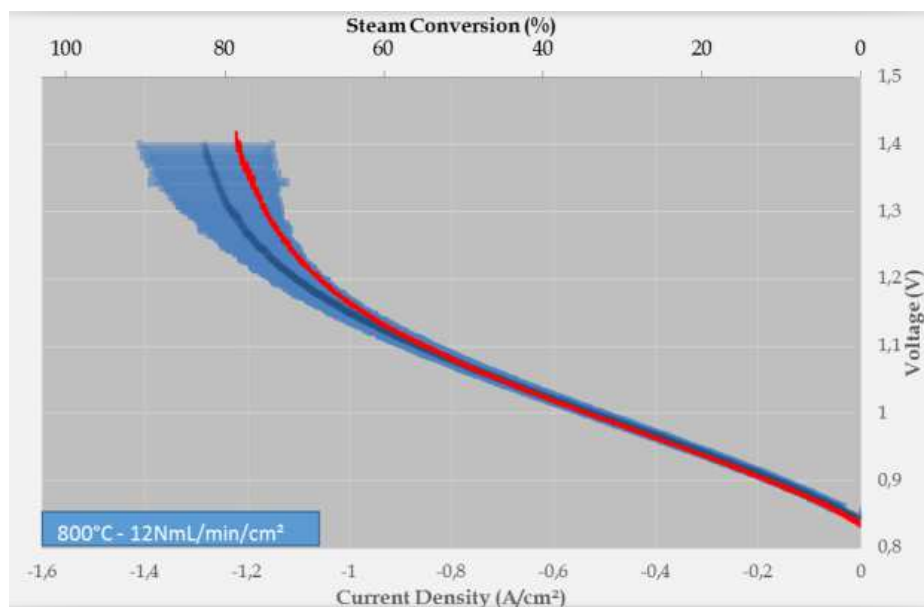

Figure 4. i-V curve representative of 200 cm² cell (red) compared to a large number of 9 cm² cells (blue); T=800 °C, total flow rate 12 NmL min^{-1} cm^{-2} of 90/10 vol.% H_2O/H_2 mix at the fuel electrode, air on the other side.

Stacks

CEA has developed a stack integrating electrode supported cells, the reference size being 12 x 12 cm, with 100 cm² active area. It is composed of 25 cells and so-called 25-100 stack (22). It is based on thin interconnects using 0.2 mm AISI441 ferritic stainless steel sheets. A nickel-mesh and an LSM (lanthanum-strontium manganite) contact element are set between the cell and the interconnect in the H_2 and O_2 compartments respectively. The fluidic design is a cross flow path. Sealing is achieved with a commercial ceramic glass. A mica foil is added to ensure the electrical insulation between two adjacent interconnects, but also to complete the sealing and to precisely position the cell. First stack optimizations were performed in order to increase the steam conversion on hydrogen side, decrease the pressure drops and allow higher flow rates especially on oxygen side (23-24). This design can accommodate cells from different providers. For instance, it has successfully integrated Elcogen cells (4,24), CEA cells, and also DTU cells (25). Regarding stack upscaling activities, first the size of the cells has been increased, from 100 to 200 cm² active area (4), and on the other hand the number of cells per stack, from 25 to 50 and 75 (5-6). Stacks made of 25, 50 or 75 cells of 200 cm² are so-called 25-200, 50-200 and 75-200 stacks.

Over the last ten years, CEA has produced 88 stacks as reported in figure 5. Most of them are 25-100 reference stacks, with a large increase of their number in 2020. It is worth noticing that CEA has put in operation its pilot workshop in 2019, which first allowed to increase the number of stacks produced after this date, and second to decrease the scrap rate. It can indeed be noticed from figure 5 that the number of 25-100 stacks which failed remains in the range of 1 to 2 per year even when the number of stacks produced is multiplied by a factor of up to 5, which highlights a better control of the process. The preparation of 25-200 stacks and large stacks (50 and 75 cells) is more recent, starting in 2020 and increasing since 2021.
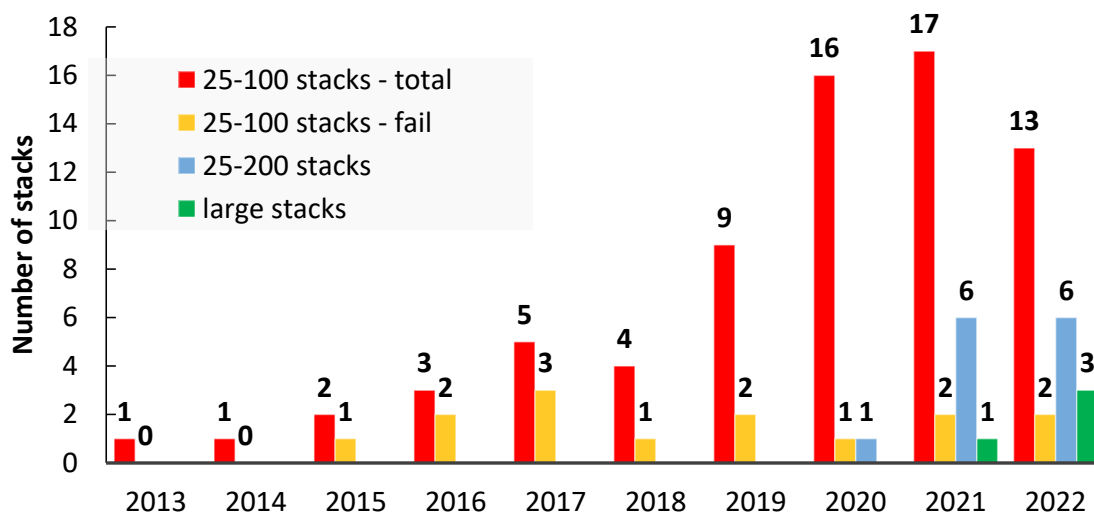
Figure 5. Number of stacks produced over years; 25-100 reference stacks in red, 25-200 stacks in blue; large stacks (50 and 75 cells in green); for the 25-100 reference stacks, the share of stacks which failed is provided.

Large 50 and 75-cell stacks required design modification to allow feeding the stack with flow rates multiplied by a factor of up to 6 as compared to the reference one, and to insure a good homogeneity of fluidic distribution to all cells in the stack and on the surface of each cell. While the 50-200 stack is composed of 50 cells piled up, the 75-200 stack is constituted of an assembly of 3 substacks, each composed of 25 cells of 200 cm². The so-called 25-200 substacks were produced individually, reduced and tested separately in terms of initial performances before being assembled to form the 75-200 stack. The performance of the 25, 50 and 75-cell stacks are presented in figure 6. The performance of the 50-200 stack is close to the one of the reference 25-100 stack. A current density of -0.9 A cm^{-2} is achieved at 1.3 V. The performance of the best 25-200 stack is superimposed to the 50-200 stack. However, there is a certain scattering in the performances of the three 25-200 stacks, leading to a performance of the 75-200 stack a bit lower, around -0.8 A cm^{-2} is achieved at 1.3 V.
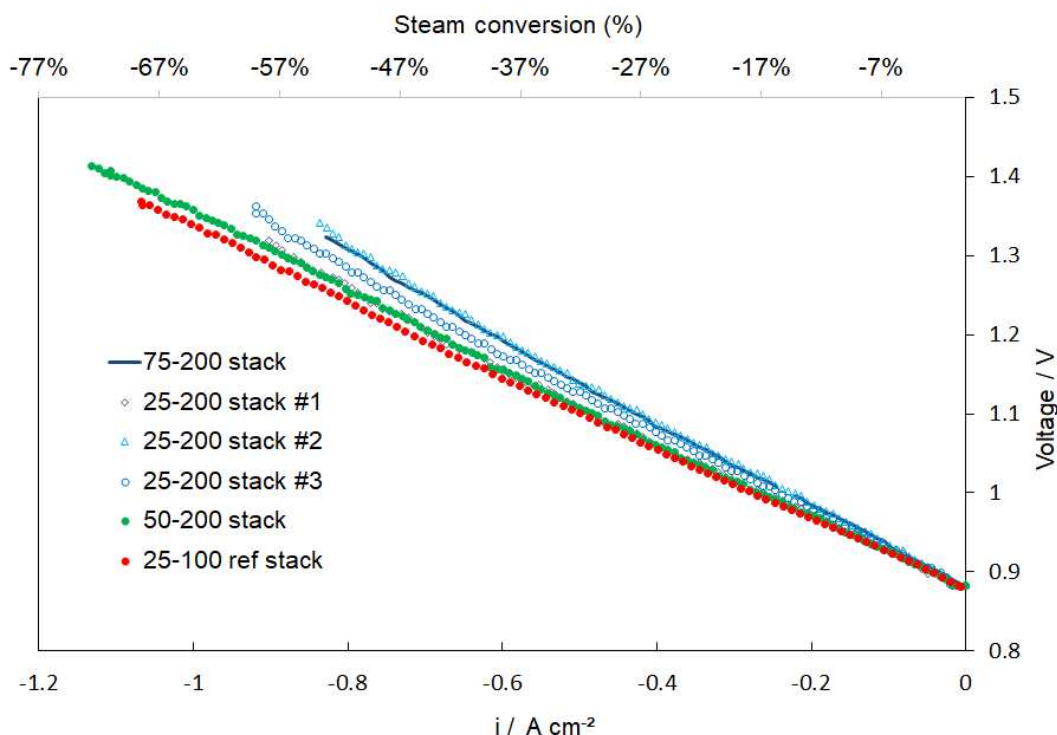

Figure 6. Comparison of the i-V curves for the different stacks; T=700 °C, total flow rate 12 NmL min^{-1} cm^{-2} of 90/10 vol.% H_2O/H_2 mix at the fuel electrode, air on the other side; 25-100 reference stack in red, three 25-200 stacks in open blue symbols; 50-200 stack in green; 75-200 stack made of the 3 25-200 stacks corresponds to the blue line

Besides performances, durability studies have been performed at different stack levels (short stack, reference 25-100 stack and 75-200 stack). For instance a 6800 h test has been performed on a 25-100 stack. The stack was galvanostatically controlled, with different current densities over the test duration and the steam conversion was kept constant at 70%. In addition, stack voltage was maintained close to the thermoneutral value (approximately 1.29 V per cell at 750 °C), to reduce thermal gradients in the stack. As a result, the only remaining parameter, the stack temperature, was adjusted so that the previous targets were met. Consequently, the stack temperature was regularly increased to compensate for the degradation and maintain the cells in (near) thermoneutral operation. With this operation

strategy, no hydrogen production loss (the hydrogen production being directly related to the current density) has been observed over the total test duration (26-27).

The same operation strategy has been adopted for an ongoing durability test on a 75-200 stack. The stack has been operated at – 0.65 A cm^{-2}, with a steam conversion of 60%, the stack being approximately maintained at the thermoneutral voltage (in average). At the time of writing this article, the stack has been operated for 2300 h, without any hydrogen production loss (figure 7).
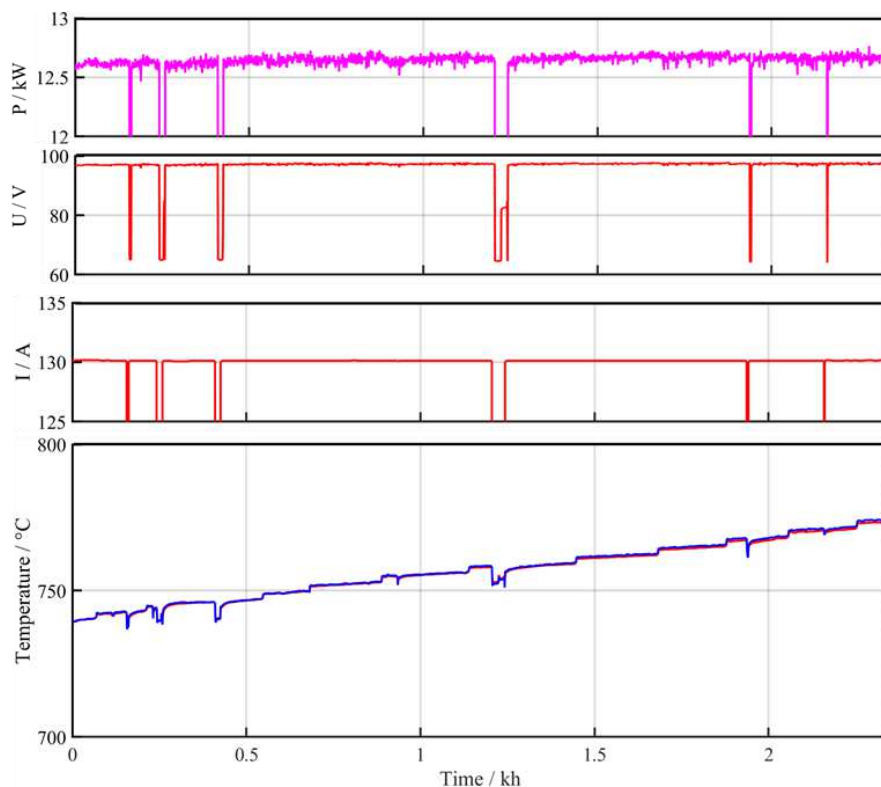

Figure 7. Time evolutions for stack current, voltage, power and outlet gas temperature during the ongoing durability test of a 75-200, 12.6 kW$_{DC}$ stack.

In parallel, improved seals have been developed to increase the stack robustness to transient operation and interconnect coatings have been implemented using different deposition techniques. Several coatings, based on Ce and Co layers, combined in various ways (see figure 8), have been deposited as thin layers (about 50 and 600 nm respectively) on samples by PVD-HiPIMS. Oxidation resistance, Cr evaporation and ASR measurements at high temperatures have been performed over durations up to 5000 h. CeCo-based coatings have been found to be efficient to reduce the oxidation kinetics compared to bare AISI441 material. They are also very efficient in reducing Cr evaporation from the AISI441 steel after 5000 h in air at 700 and 800 °C. Indeed, a very low Cr amount is detected in a getter material facing coated samples, showing a 67-74% and 71-78% efficiency compared to bare AISI441 alone at 700 and 800 °C respectively (figure 8). After the validation of the coatings at sample scale, the CeCo coating has been integrated into a 9-cell stack. This stack comprises some interconnects coated on oxygen side (repeating units RUs 2, 4, 6 and 8) and has been tested over 5000 h (figure 9). In average, results show lower or equal degradation rates for coated RUs than for uncoated ones (including or excluding the extreme RUs from the calculation where thermal and gas distribution effects can appear),

based on evolutions of voltage, ASR from i-V curves and polarization resistance recorded using Electrochemical Impedance Spectroscopy. Nevertheless, the improvement brought by the CeCo coating appears less strong at this short stack scale in the selected operating conditions, than from testing at sample scale. This could be explained by an effect of the stack environment, and in particular the contact layer which might play a protecting role. Also the weaker Cr poisoning of O_2 electrodes in SOEC operation recently mentioned in literature could contribute to this lower apparent improvement (28).
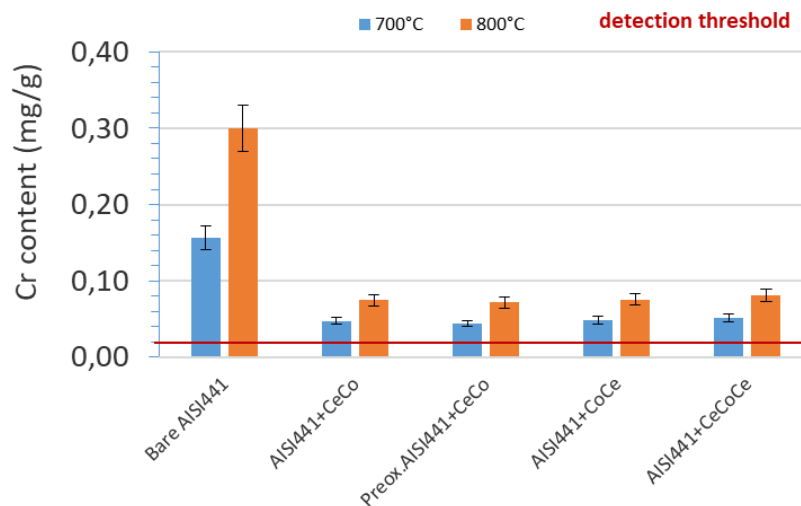

Figure 8. Cr concentration measured by ICP-OES in a getter material facing the samples oxidized 5000 h at 700 and 800 °C in static air. Vertical black intervals represent the 10% dispersion of each average value, obtained with this technique.
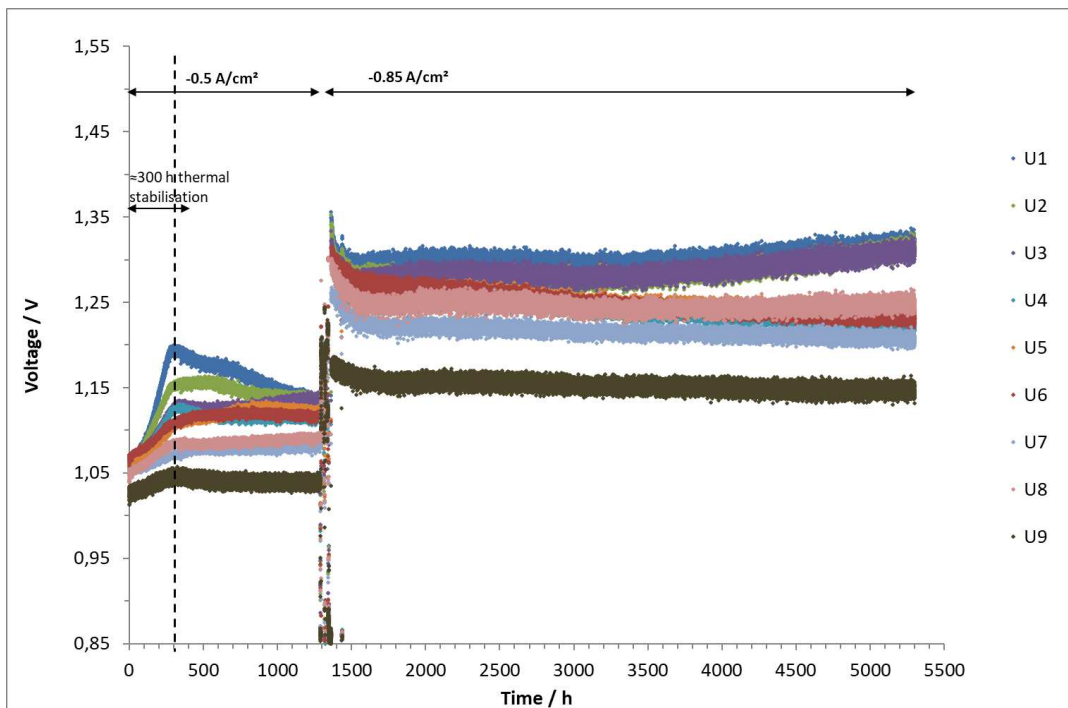

Figure 9. Voltage evolution of the 9 RUs of the stack, recorded at 750 °C and 12 NmL min^{-1} cm^{-2} of 90/10 vol.% H_2O/H_2 mix at the fuel electrode, air on the other side. Odd RUs in standard configuration. Even RUs with CeCo-coated interconnect on the O_2 side. A first step was performed at – 0.5 A cm^{-2}, a second at – 0.85 A cm^{-2}.

Modules

CEA has put in operation a test platform able to operate modules with a power up to 120 kW$_{DC}$, in electrolysis and fuel cell mode (29). A 4-stack module has been designed, assembled and put in operation (30). Made of four 25-100 stacks, it is able to operate in electrolysis, fuel cell and reversible mode. After manufacturing and assembly, functional tests have been performed, first with no stacks (possibility to test module fluidic and thermal functionalities by connecting gas inlets and outlets) then with dummy stacks and finally with actual 25-100 stacks. The first electrochemical tests have started with 2 stacks plus 2 dummy stacks. The initial performances of the two stacks, supplied in gas by common rail and operated at same current, are similar to the ones recorded during the stack manufacturing, and are perfectly superimposed, which confirm the good fluidic distribution between the stacks in the module and the well uniform temperature in the hotbox. A durability test has been started, with a current density of $-$ 0.65 A cm^{-2}, and a steam conversion of 70%. The operation strategy was as above and as reported in (26-27), to operate at the thermoneutral voltage and to compensate the degradation by a temperature increase. The evolution of the temperature of the hotbox (the same for the two stacks) is reported in figure 10, and compared to the initial step of the 25-100 stack tested during 6800 h, operated in the same conditions and reported in (26-27). One can see a very good superposition of the two curves, demonstrating the good and reproducible operation of the two stacks in the hotbox (30).
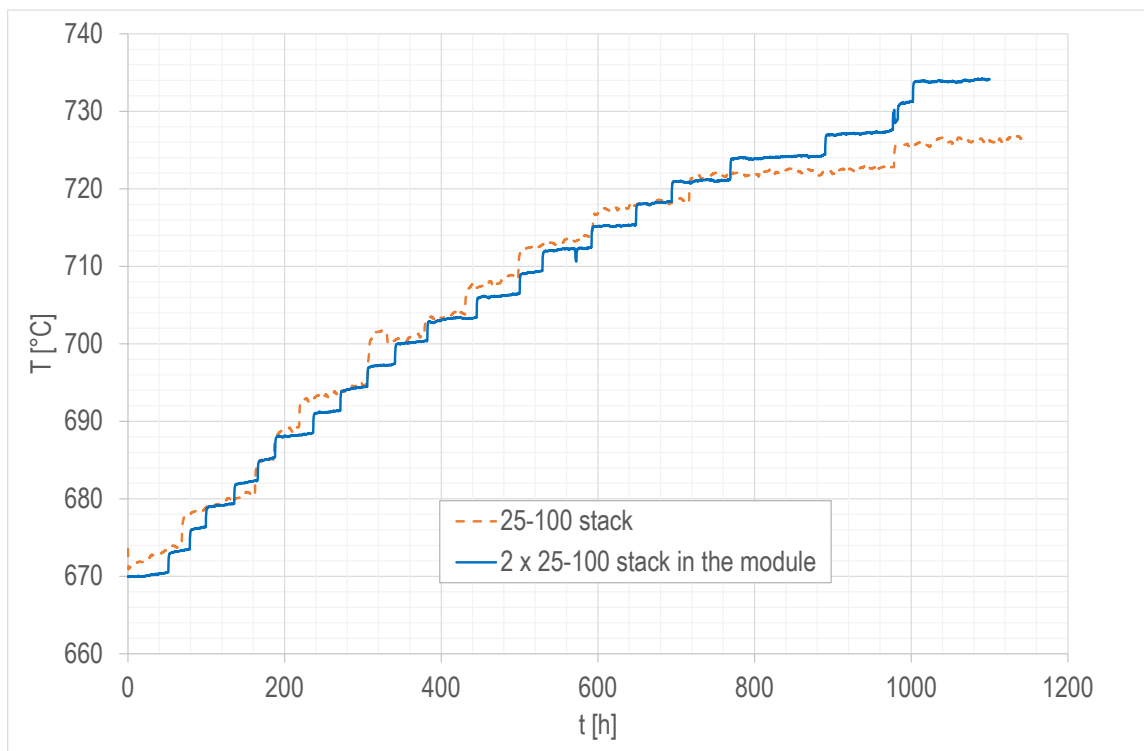

Figure 10. Time evolutions for temperature of the hotbox in which the two stacks are operated at $-$ 0.65 A cm^{-2}, and a steam conversion of 70% to be close to the thermoneutral voltage; comparison with the reference 25-100 stack as published in (26-27)

Conclusions

An overview of CEA activities on SOC technology has been presented, with a focus on the recent achievements regarding performance and durability at the different scales of cells, stack components, in particular coatings, stacks and modules. First, developments performed to obtain cells with improved performances and a larger surface have been reported, with a methodology combining multiscale and multiphysics modelling, electrochemical characterization in relevant conditions and advanced post-test analysis. As far as stack developments are concerned, CEA continued its program on upscaling, and a long-term test on a large stack is presented. In parallel, interconnect coatings were developed and integrated in a stack for long-term durability test after validation at sample level. Finally, a 4-stack module has been designed and its first thousand hours of operation are reported.

Acknowledgments

References

1. European Commission, *The European Green Deal*, can be found under https://commission.europa.eu, **2019**.
2. A. Chatroux, M. Reytier, S. Di Iorio, C. Bernard, G. Roux, M. Petitjean, and J. Mougin, *ECS Trans.*, **68**(1), 3519 (2015).
3. J. Mougin, J. Laurencin, J. Vulliet, S. Di Iorio, G. Roux, M. Reytier, and F. Lefebvre-Joud, 12th European SOFC&SOE Forum 5-8 July 2016, Luzern, A0605 (2016).
4. G. Cubizolles, J. Mougin, S. Di Iorio, P.Hanoux, and S. Pylypko, *ECS Trans.*, **103**(1) 351 (2021)
5. S. Di Iorio, T. Monnet, G. Palcoux, L. Ceruti, and J. Mougin, 15th European SOFC&SOE Forum 5-8 July 2022, Luzern, A0904 (2022)
6. S. Di Iorio, T. Monnet, G. Palcoux, L. Ceruti, and J. Mougin, *Fuel Cells*, in press (2023)

7. Clean Hydrogen Partnership, *Strategic Research and Innovation Agenda 2021 – 2027,* can be found under https://www.clean-hydrogen.europa.eu/about-us/key-documents/strategic-research-and-innovation-agenda_en, **2022**

8. E. Da Rosa Silva, G. Sassone, M. Prioux, M. Hubert, B. Morel, and J. Laurencin, *J. Power Sources* **556** 232499 (2023).

9. G. Sassone, E. Da Rosa Silva, M. Prioux, M. Hubert, B. Morel, A. Léon, and J. Laurencin, submitted to *ECS Trans.* (2023)

10. A. Abaza, S. Meille, A. Nakajo, D. Leguillon, M. Hubert, C. Lenser, and J. Laurencin, ECS Trans. **103** 1151 (2021).

11. C. Hartmann, J. Laurencin, G. Geneste*, Physical Review B,* **107**(2), 024104 (2023).

12. F. Monaco, E. Effori, M. Hubert, E. Siebert, G. Geneste, B. Morel, E. Djurado, D. Montinaro, and J. Laurencin, *Electrochimica Acta,* **389,** 138765 (2021).

13. E. Effori, J. Laurencin, E. Da Rosa Silva, M. Hubert, T. David, M. Petitjean, G. Geneste, L. Dessemond, and E. Siebert, *J. Electrochem. Soc.*, **168** 044520 (2021).

14. G. Sassone, O. Celikbilek, M. Hubert, K. Develos-Bagarinao, T. David, L. Guetaz, I. Martin, J. Villanova, L. Rorato, B. Morel, A. Léon, and J. Laurencin, submitted to *ECS Trans.* (2023)

15. F. Monaco, M. Hubert, J. Vulliet, J.P. Ouweltjes, D. Montinaro, P. Cloetens, P. Piccardo, F. Lefebvre-Joud, and J. Laurencin, J. Electrochem. Soc., **166** (15) F1229 (2019)

16. L. Rorato, Y. Shang, S. Yang, M. Hubert, K. Couturier, L. Zhang, J. Vulliet, M. Chen, and J. Laurencin, Accepted in J. *Electrochem. Soc.* (2023) DOI 10.1149/1945-7111/acc1a3.

17. J. Laurencin, M. Hubert, K. Couturier, T. Le Bihan, P. Cloetens, F.Lefebvre-Joud, and E.Siebert, *Electrochimica Acta*, **174**, 1299 (2015).

18. M. Hubert, J. Laurencin, P. Cloetens, J.C. da Silva, F. Lefebvre-Joud, P. Bleuet, A. Nakajo, and E. Siebert, *Solid State Ionics*, **294**, 90 (2016).

19. E. Effori, H. Moussaoui, F. Monaco, R. K. Sharma, J. Debayle, Y. Gavet, G. Delette, G. Si Larbi, E. Siebert, J. Vulliet, L. Dessemond, and J. Laurencin, *Fuel Cells*, **19**(4) 429 (2019).

20. H. Moussaoui, J. Laurencin, Y. Gavet, G. Delette, M. Hubert, P. Cloetens, T. Le Bihan, and J. Debayle, *Comput. Mater. Science* **143**, 262 (2018).

21. H. Moussaoui, R.K. Sharma, J. Debayle, Y. Gavet, G. Delette, and J. Laurencin, *J. Power Sources* **412**, 736 (2019).

22. M. Reytier, S. Di Iorio, A. Chatroux, M. Petitjean, J. Cren, M. De Saint Jean, J. Aicart, and J. Mougin, *Int. J. of Hydrogen Energy*, **40**, 11370 (2015).

23. J. Mougin, S. Di Iorio, A. Chatroux, T. Donnier-Marechal, G. Palcoux, M. Petitjean, and G. Roux, *ECS Trans.*, **78**(1) 3065 (2017)

24. A. Ploner, A. Hauch, S. Pylypko, S. Di Iorio, G. Cubizolles, and J. Mougin, *ECS Trans.*, 91, 2517 (2019).

25. V. Saarinen, J. Pennanen, M. Kotisaari, O. Thomann,1 O. Himanen, S. Di Iorio, P. Hanoux, J. Aicart, K. Couturier, X. Sun, M. Chen, and B. R. Sudireddy, *Fuel Cells*, **21**, 477 (2021).

26. J. Aicart, A. Surrey, L. Champelovier, K. Henault, C. Geipel, O. Posdziech, and Julie Mougin, accepted, *Fuel Cells*, in press (2023).

27. J. Aicart, A. Surrey, L. Champelovier, K. Henault, C. Geipel, O. Posdziech, and Julie Mougin, 15th European SOFC&SOE Forum 5-8 July 2022, Luzern A0804 (2022)

28. Z. Zhu, M. Sugimoto, U. Pal, S. Gopalan, and S. Basu, *J. Power Sources*, **471** 228474 (2020).
29. J. Aicart, Z. Wuillemin, B. Gervasoni, D. Reynaud, F. Waeber, C. Beetschen, Y. Antonetti, A. Nesci, and J. Mougin, *Int. Journal of Hydrogen Energy*, **47**, 3568 (2022).
30. G. Cubizolles, S. Alamome, F. Bosio, B. Gonzalez, C. Tantolin, L. Champelovier, S. Fantin, and J. Aicart, submitted to *ECS Trans.* (2023).